Detailed Kinetic Modeling for the Pyrolysis of a Jet A Surrogate

Authors names

Florence H. Vermeire[1], Syam Ukkandath Aravindakshan[2], Agnes Jocher[1], Mengjie Liu[1], Te-Chun Chu[1], Ryan E. Hawtof[1], Ruben Van de Vijver[2], Matthew B. Prendergast[1], Kevin M. Van Geem[2], William H. Green[1,*]

Authors affiliations

[1]Department of Chemical Engineering, Massachusetts Institute of Technology, 77 Massachusetts Ave., Cambridge, MA 02139, United States of America

[2]Laboratory for Chemical Technology, Ghent University, Technologiepark 125, 9052 Gent, Belgium

[*] Corresponding author: whgreen@mit.edu

Keywords

Automatic kinetic modeling, Jet A surrogate, Reaction Mechanism Generator, Pyrolysis, Cross-chemistry

Highlights

- Automatic kinetic model generation with RMG for a multi-component surrogate mixture of Jet A
- New experimental data for Jet A surrogate pyrolysis in a tubular reactor with detailed product analysis
- Importance of cross-chemistry demonstrated with rate-of-production and sensitivity analyses

Abstract

Fuel microchannels for regenerative cooling are receiving increased attention in advanced aviation technologies. Those microchannels allow heat integration between the endothermic cracking of the jet fuels and their subsequent combustion. In this work, a detailed elementary-step kinetic model is developed to gain insights in the cracking chemistry of a Jet A surrogate (*n*-dodecane, isooctane, *n*-propyl benzene, and 1,3,5-trimethylbenzene), which allows for further optimization of those aviation technologies. A dedicated procedure is described for the automated generation of kinetic models for multi-component mixtures with the open-source Reaction Mechanism Generator (RMG) software. The full kinetic model is validated against experimental measurements in multiple reactor geometries, at various experimental conditions, including both a surrogate mixture and commercial Jet A. The experimental data includes new experimental measurements for the pyrolysis of a Jet A surrogate in a tubular reactor with detailed product analysis using comprehensive 2D GC. The good performance of the kinetic model for data from a broad range of experimental conditions demonstrates the advantage of a kinetic model with detailed chemistry against empirical kinetic models that are limited in their applicability range. Further analysis of the important chemistry in the kinetic model shows that it is essential to account for cross-reactions between the different surrogate components.

1. Introduction

The continued drive to advance aviation technologies over recent years has created an increased demand for improved propulsion systems with better performance and efficiency. One technology that has seen an increasing interest is the fuel microchannel for regenerative cooling.[1,2] This technology utilizes endothermic cracking of the jet fuel prior to combustion as a heat sink for aerodynamic heating of the aircraft. To improve our understanding on the thermodynamics of the regenerative cooling system, improvements in the modeling of fuel cracking are required. Jet fuels, generally mixtures of varying types and weights of hydrocarbons, have complex cracking mechanisms that make accurate heat sink predictions difficult. The general approach to handling such large cracking mechanisms is a combined experimental and computational approach that generates empirical, lumped, and simplified cracking mechanisms from experimental results. This approach results in a model that is limited to specific fuel compositions and the range of experimental conditions covered. The cracking mechanisms developed with those approaches cannot be used with full confidence in a broader set of experimental conditions. One example of one of the most advanced empirical cracking mechanisms for jet fuels is HyChem, recently developed by Wang et al.[3,4] The pyrolysis of jet fuels is modeled with seven lumped reactions where stoichiometry and reaction rates are derived from experimental data. The pyrolysis model is combined with a more detailed oxidation model for the pyrolysis products to predict oxidative pyrolysis of jet fuels.

For this work, we use the open-source automatic kinetic model generation tool named Reaction Mechanism Generator (RMG)[5,6] to develop a detailed kinetic model for the pyrolysis of a Jet A surrogate. We demonstrate a new approach to the construction of chemical kinetic models for complex fuels without fitting of any of the model parameters to experimental data. This way, it can be reliably applied to kinetic simulations of varying reactor geometries and experimental conditions. This approach is demonstrated for a Jet A surrogate (2nd generation surrogate with *n*-dodecane, isooctane, *n*-propyl benzene, and 1,3,5-trimethylbenzene (TMB))[7], but can be adopted for other complex multi-component hydrocarbon mixtures as well. For validation of the novel kinetic model, experimental data is gathered for pyrolysis of the specific surrogate composition, rich in aromatic components, in a tubular reactor with a detailed analysis section. Additionally, the kinetic model is used to simulate literature data on the pyrolysis of a commercial Jet A in a shock

tube.[8] By validating the kinetic model against a broad range of experimental conditions in various reactor geometries, we show the advantage of a fuel-specific yet geometry independent kinetic modeling procedure that can offer more realistic insights in the chemical behavior than simplified empirical models.

2. Selection of the surrogate composition

Jet fuels are highly complex mixtures of many organic species with a composition that often varies between samples within a given fuel classification. The individual components in samples of Jet A specifically have been found to vary by as much as 25%.[9] Both the large number of relevant species as well as the variance in composition make modeling fuel behavior very difficult. For modeling efforts to succeed, fuel surrogates that meet certain performance and compositional standards are often adopted.

An effective fuel surrogate fuel typically has no more than a dozen initial components, with some surrogates using as few as 3 to 5 components or even a single species. Furthermore, an effective surrogate fuel must be able to approximate certain physical properties of the real fuel, including the hydrogen to carbon (H/C) ratio, sooting/coking behavior, reaction potential as represented by the Derived Cetane Number (DCN), and the average molecular weight.[10]

Several strategies have been investigated in literature for quick and efficient identification of viable surrogates, including one method by Dooley et al.[11] that seeks to emulate the desired physical properties through correlation of the surrogate and original fuel molecular fragments. The resulting surrogate, a mixture of *n*-decane, isooctane, and toluene, was computationally compared to a specific Jet A sample (POSF-4658).[11] During the development of this first generation surrogate, kinetic models for each of the primary components as well as supplementary models for ethane, butadiene, and similar species were used but cross-reactions were not considered due to lack of comprehensive literature mechanisms on the subject. Good agreement was found for post-combustion species such as carbon monoxide and carbon dioxide when the surrogate model was computationally compared to experimental results from a variable pressure flow reactor.[11]

The success of a first generation POSF-4658 surrogate led to further development and the generation of more complicated second generation surrogates. The second generation surrogate utilizes *n*-dodecane as a primary alkane species instead of *n*-decane, keeps a revised isooctane

model, and removes toluene in favor of *n*-propyl benzene and 1,3,5-trimethylbenzene.[7,12] Combustion experimental data was collected in a high pressure shock tube for both Jet A and the new surrogate fuel in a high pressure shock tube. Post-combustion products for both fuels were compared and good agreement was found for mole fractions of carbon monoxide, carbon dioxide, light species with one to three carbons, and ignition delay times at temperatures ranging between 879–1733 K and pressures between 16–27 atm.[7] Further, the second generation surrogate was shown to have very similar physical properties and sooting behavior, as is shown in Table 1.

Table 1. Comparison of physical and sooting properties by Dryer et al.[10] DCN: Derived Cetane Number, TSI: threshold sooting index, MW: average molecular weight.

Fuel	DCN	H/C	MW (g/mol)	TSI
Jet A	47.1	1.95	157.5	24.2
1st gen surrogate[11]	47.4	2.01	120.7	14.1
2nd gen surrogate[12]	48.5	1.95	138.7	20.4

For the selection of the Jet A surrogate used in this work, we recognize the effectiveness of the second generation surrogate proposed by Dooley et al.[12] But also the underlying design principle for both first and second generation surrogates, *i.e.* the importance of functional groups in the selection of surrogate components as stated by Dooley et al.[12], are considered important for the final surrogate selection. The surrogate composition used in this work is enriched in aromatic components compared to the surrogate reported by Dooley et al.[12] and has a molar composition of 0.287/0.235/0.404/0.074 for *n*-dodecane/isooctane/*n*-propyl benzene/TMB.

3. Automate kinetic modeling for multi-component mixtures

A kinetic model for the pyrolysis of the Jet A surrogate was developed using the Reaction Mechanism Generator (RMG).[5,6] RMG is an open-source software package built to automatically generate chemical kinetic models for gas-phase reactive systems. In the past RMG has mostly been applied to systems with simple initial compositions (e.g. a single-component fuel, or a mixture of

small molecules). In this work, we demonstrate how RMG can be used for model development of a complicated multi-component surrogate mixture. First, we give a general overview of how RMG generates kinetic models and calculates thermodynamic and kinetic properties. Kinetic models were generated and validated for the individual components in the surrogate mixture. RMG was then used to generate cross-reactions between the individual component models and the final model is merged from the individual models.

Note that this specific approach is employed rather than generating a model for the complete surrogate mixture at all the reaction conditions of interest in a single RMG run. Although that approach would hypothetically allow RMG to explore the interactions between all of the surrogate components and intermediates, in this work we discovered that RMG was not able to handle that level of complexity, at least on the computer hardware we employed. As shown below, the chemistry of each of the four individual components in the surrogate mixture is by itself complex and requires identifying and accounting for thousands of species and their reactions. RMG attempts to exhaustively consider every possible species and reaction to reduce the likelihood of omitting one that is important. As a consequence, the number of potential species and reactions considered is orders of magnitude larger than the number actually included in the final model. Also, at each iteration RMG solves the current version of the model at all the reaction conditions of interest. This stiff-ODE solution is very fast for small models, but when the model grows and contains thousands of species this step becomes time-consuming. Even with several algorithmic improvements and partial parallelization of the software, the memory and CPU requirements for constructing the model climb steeply as the model becomes more complex.

In this work, we hit the limit of what could be done with this version of RMG and our computer resources, so were forced to build the model in pieces rather than all at once. We note that manual construction of kinetic models is typically done, by combining sub-models in a similar way. This is much faster than attempting to build a comprehensive model, but as discussed below it introduces new difficulties, e.g. how to correctly add the reactions that connect the different sub-models.

3.1. Automated kinetic model generation with RMG

The framework of RMG has been discussed in detail before[5,6] and documentation is available on the RMG website.[13] Below, a short overview of the main functionalities that are important to this work is given.

The automatic kinetic model generation in RMG is done step-wise with a rate-based criterion. The mechanism is generated from a pool of initial reactants, a set of reactor conditions, and more than 45 pre-defined reaction families. RMG distinguishes the core and the edge mechanism. The core mechanism contains all important species and the reactions between those species. Those species and reactions comprise the final mechanism. The edge mechanism contains new species that can be formed from the core species using the RMG reaction families and libraries. During every iteration, the edge species formed with the highest flux at the predefined reactor conditions is added to the core mechanism. This procedure continues until a user-specified termination criterion on the conversion of components or batch residence time is met. Some additional constraints can be set to limit the size and number of edge species.

In order to perform reactor simulations at every iteration, thermodynamic properties are required for each species and kinetic parameters are required for each reaction in the kinetic model. Some of these parameters are known from prior work, and are stored in libraries, but most need to be estimated. For fast estimation of thermodynamic properties, RMG uses the Benson group additivity method with many of the group values derived from quantum chemical calculations.[14,15] For kinetics each reaction is classified using a hierarchical tree, and then assigned high-pressure-limit Arrhenius parameters derived from other similar reactions (with those numbers typically coming from transition state theory calculations).

After automatic generation of the preliminary kinetic model with RMG, the resulting model is used for reactor simulations and comparison to experimental data. Discrepancies with experimental measurements are identified and model analysis tools are used to identify sensitive species and reactions resulting in those discrepancies. For those species and reactions, more accurate thermodynamic and kinetic properties are determined, for example by using the CBS-QB3 method.[16,17] The new calculations are added to the RMG database and a new kinetic model incorporating them is generated. If the original estimates were very different from the CBS-QB3 values, the new reaction network might be significantly different than the original model. This can

be the case, for example, because a particular reactive intermediate is now predicted to be formed at a much higher rate, so its reactions need to be included. This procedure is repeated many times to try to converge to a model that includes all the important species and reactions, where all the sensitive parameters in the model are derived from high-level calculations rather than rough estimates [18,19].

Because the chemistry is very complex, there are a huge number of rate coefficients in the model, many more than the number of available experimental data. The goal here is to understand how well we can predict complex chemistry from fundamental understanding, not how well one can fit limited experimental data. We emphasize that none of the many rate coefficients and thermodynamic parameters in the model were adjusted to try to fit the data shown below; the numbers in the models are the Benson-type estimates made automatically by RMG, or the more accurate numbers from specific quantum chemistry calculations. However, in a few cases we observed that RMG had misestimated the symmetry numbers of some molecules or related reaction-path degeneracies by a factor of 2, and we corrected those particular numbers by hand.

3.2. Single component modeling and validation

The procedure explained above was used to generate kinetic models for the individual surrogate components: *n*-dodecane, isooctane, *n*-propyl benzene, and TMB. Each of those kinetic models are used for simulations to compare to literature-based experimental measurements at various conditions. For each of the components, the RMG databases are updated with more accurate CBS-QB3 calculations for important species and reactions. The most important observations and updates during the kinetic model construction of the individual surrogate components are discussed below.

The kinetic modeling efforts for *n*-propyl benzene pyrolysis are an excellent example of how replacing estimated rate and thermochemical parameters in large kinetic models with more accurate values from quantum chemistry calculations improves model performance. The pyrolysis of *n*-propyl benzene was studied experimentally by Gudiyella and Brezinsky[20] in a shock tube with temperature ranging from 1027 to 1678 K and a pressure of 50 atm. Those experiments were used to compare the kinetic model simulations, identify discrepancies, and improve thermodynamic properties and kinetics for the most important species and reactions. Simulations with the first kinetic model showed poor agreement for the *n*-propyl benzene conversion profile. The pyrolysis

initiation temperature was off by ~60–70 K. Sensitivity analysis on the model indicates which parameters control the decomposition temperature, so we replaced the estimated value for those key parmeters with more accurate numbers computed using quantum chemistry. The thermodynamics and kinetics libraries were updated with new calculations or by data available from literature calculated by Darcy et al.[21] The new calculations are performed at the CBS-QB3 level of theory [16,17] as implemented in the Gaussian 16 [22] software. Post-processing of the quantum calculations to thermodynamic properties and rate coefficients is done with the open-source software Arkane [23,24]. This process of using sensitivity analyses to identify which parameters should be computed using quantum chemistry was repeated for several observables. The final model, built by RMG using these more accurate values for the key parameters, captures the *n*-propyl benzene conversion as a function of temperature accurately. The performance against experimental data by Gudiyella and Brezinsky[20] can be found in the Supporting Information (Figure S1). The shock tube experimental data is only used to determine the key model parameters and none of the model parameters are fitted to the experimental data. With this method, a kinetic model is developed that is valid for a wide range of process conditions. To evaluate the performance of the kinetic model at different conditions, simulations for *n*-propyl benzene pyrolysis are done to model the experiments performed by Chen and Froment[25] in a tubular reactor. Without any parameter adjustment, a good agreement is obtained between model simulations and experimental data as can be seen Figure 1.

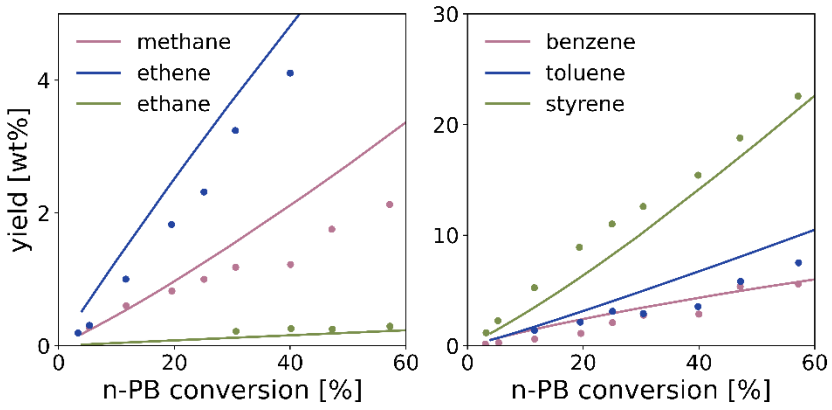

Figure 1. Performance of the kinetic model for *n*-propyl benzene pyrolysis against experimental data reported by Chen and Froment[25] in a tubular reactor. Product yields (wt%) are plotted as a function of *n*-propyl benzene (*n*-PB) conversion.

The same method, using sensitivity analysis on rough models to identify which parameters should be computed using quantum chemistry, then automatically rebuilding the model with RMG was

used to construct a model for the pyrolysis of *n*-dodecane. Many have reported experimental data for *n*-dodecane pyrolysis. Two experimental datasets were selected for comparison to the kinetic model in this work, *i.e.* the jet-stirred reactor experiments reported by Herbinet et al.[26] and the shock tube experiments reported by Malewicki et al.[27] Those experimental datasets cover two different reactor types, a broad range of experimental conditions, and both studies report detailed product profiles. The jet-stirred reactor experiments reported by Herbinet et al.[26] were done at atmospheric pressure and temperatures ranging between 800 and 1075 K. Shock tube experiments reported by Malewicki et al.[27] were at pressures 25 and 50 atm, and temperatures between 900 and 1700 K. Simulation results are compared against the experimental reaction profiles of the major products as a function of temperature in Figure 2 for the jet-stirred reactor experiments. A comparison of the model predictions with the shock tube experimental data is given in the Supporting Information (Figure S2 and S3). The model predictions are in good agreement with both sets of *n*-dodecane pyrolysis experiments.

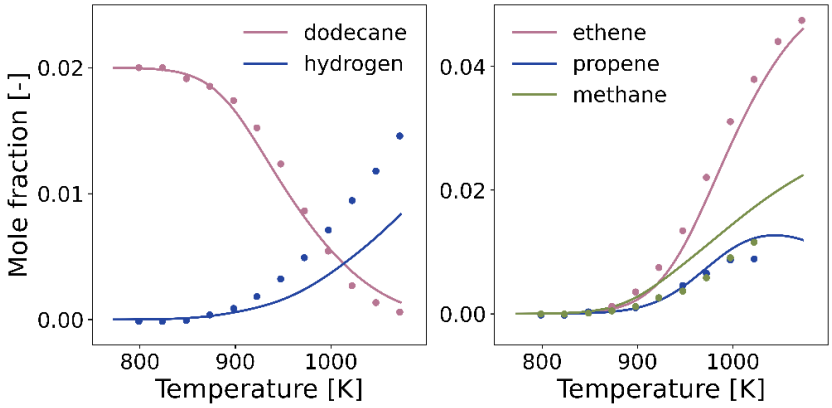

Figure 2. Performance of the kinetic model for *n*-dodecane pyrolysis against experimental data reported by Herbinet et al.[26] measured in a jet-stirred reactor.

The same procedure was used to replace the key parameters in the model for the pyrolysis of isooctane (2,2,4-trimethylpentane) with more accurate quantum chemical values. Experimental validation, see Figure 3, is done with the high-pressure single pulse shock tube experiments reported by Malewicki et al.[28] The experimental measurements were done at 26 and 55 atm, for temperatures ranging from 835 to 1757 K.

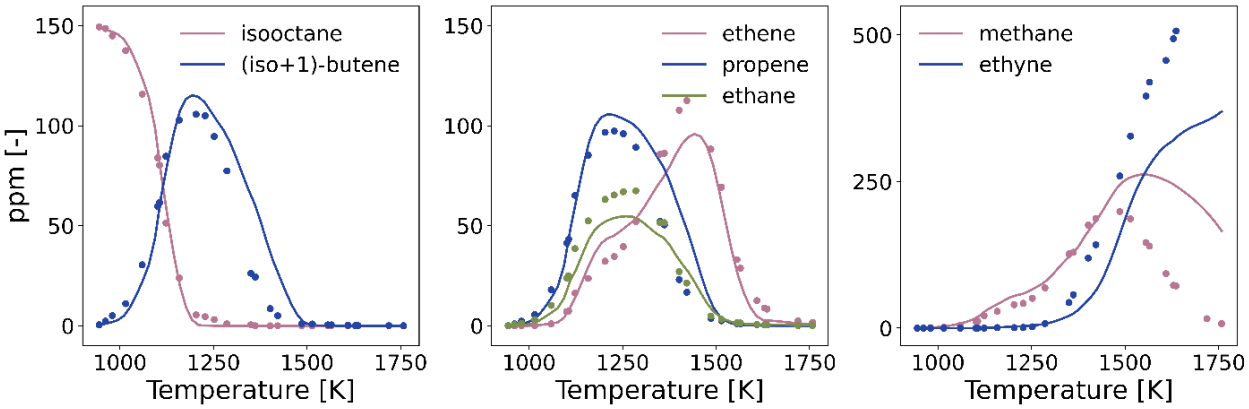

Figure 3. Performance of the kinetic model for isooctane pyrolysis against experimental data reported by Malewicki et al.[28] in a shock tube reactor.

While no RMG model showed sufficient agreement after the first run, the iterative loop of mechanism generation – sensitivity analysis – quantum chemistry – mechanism generation significantly improved the model predictions in all three cases. It is not feasible to compute all the rate coefficients and thermodynamic parameters in these large kinetic models using high-level quantum chemistry methods. Only computing the most sensitive parameters affecting the observables of interest, as done here, drastically reduces the computational requirements.

The number of species and reactions for each final single-component mechanism can be seen in Table 2.

Table 2. Number of species and reactions found in the kinetic models for the pyrolysis of the individual surrogate components

Single Component	# of Species	# of Reactions
n-dodecane	438	12510
Isooctane	195	5445
n-propyl benzene	1038	9490
1,3,5-trimethylbenzene	746	11734

3.3. Generation of the full kinetic model

One can simply combine these 4 single-component models to make a rough model for the surrogate. However, a model built this way omits some of the cross-reactions between the different surrogate fuel components and their major products. To try to correct this omission, RMG is used to automatically generate some of the cross-reactions between the different surrogate components. The surrogate components are used as input to RMG, as if one were intending to use RMG to directly build the full model from scratch, but the model-construction process was only converged to loose tolerances to avoid overwhelming the computer. To further reduce memory demands a limit was set on the maximum number of carbon atoms that are allowed in the newly formed species in the edge mechanism. Further research is needed in how to optimally fill in the important missing reactions and species to correctly connect two sub-models. The cross-chemistry sub-model contains 381 species and 6791 reactions, some of which are already present in the kinetic models of the individual components.

Finally, since we want to model polycyclic aromatic hydrocarbon formation from the surrogate, which is vital for accurately modeling the coking or soot behavior, we included the aromatic formation sub-model recently compiled by Liu et al. [29] That aromatic sub-model contains 329 species and 509 reactions.

Then, the six kinetic models (four single components, one cross chemistry, and one aromatics) were merged together. The merging procedure is automated with RMG. During the merging procedure of two kinetic models, one of the models is defined as the primary, while the other model is defined as the secondary model. All species and reactions from a secondary model that do not appear in the primary are added to the primary. If duplicate species and reactions are present between the primary and the secondary model, those present in the primary are retained. In this work, the kinetic models were merged together in the following order: (1) the cross-chemistry, (2) *n*-dodecane mechanism, (3) isooctane mechanism, (4) *n*-propyl benzene mechanism, (5) TMB mechanism, (6) aromatic mechanism. This sequence is selected based on user experience and by considering the most reliable recent kinetic and thermodynamic parameters in the RMG database, the knowledge on the pyrolysis chemistry of individual components, and the degree of validation of individual kinetic models. The final kinetic model after merging contains 2774 species and 44 367 reactions. In the final model, 16% of the species thermodynamic properties and about 2% of

the reaction kinetics match entries in the RMG libraries or RMG training reactions. The other thermodynamic properties and reaction kinetics are estimated automatically by RMG as explained before. More information on the source of each individual thermodynamic and kinetic properties can be found in the commented sections of the final kinetic model in CHEMKIN format in the Supporting Information.

4. Experimental data collection

For detailed validation of the new kinetic model, new pyrolysis experiments with a Jet A surrogate mixture were performed in a tubular reactor at the bench-scale unit located at the Laboratory for Chemical Technology in Ghent University. The experimental unit has been described in detail in the past, a brief discussion specific to the new experimental data is given below. [30–32]

An aromatic-enriched surrogate Jet A mixture was prepared with *n*-propyl benzene (Fisher Scientific, 98%), *n*-dodecane (Fisher Scientific, 99%), isooctane (Fisher Scientific, >99.5%) and TMB (Fisher Scientific, >98%). The mixture had a molar composition of 40.4 mol% *n*-propyl benzene, 28.7 mol% *n*-dodecane, 23.5 mol% isooctane and 7.4 mol% TMB.

The Jet A surrogate mixture was heated and mixed with nitrogen gas before entering the reactor. The inlet mass flow rate of the surrogate mixture and nitrogen gas was 0.0003445 mol s^{-1} (1.24 mol h^{-1}) and 0.001336 mol s^{-1} (4.81 mol h^{-1}) respectively. The heater and mixer were electrically heated and filled with quartz bead units. The tubular reactor is made of Incoloy 800 HT stainless steel, has a length of 149 cm and 0.6 cm internal diameter. An external furnace is used to heat the reactor to the set temperature. The temperature was scanned between 860 K and 1080 K with 20 K increments. For simulation purposes, it is important to know the exact gas temperature profile as a function of the axial distance in the tubular reactor. The gas temperature is measured along the reactor at eight different positions with type K thermocouples. The temperature profiles as a function of the axial distance in the reactor are provided in Table S1 within the Supporting Information. The pressure in the reactor was controlled using a back-pressure regulator. During experiments the reactor pressure was set to 3 bar (300 kPa). It is found that pressure drop over the reactor is negligible; the observed pressure drop during experiments is 0.1 bar.

Downstream of the reactor, the effluent was sent through a sampling system kept at 573 K to avoid condensation. The effluent is analyzed with an on-line refinery gas analyzer (RGA) and comprehensive 2D gas chromatography (GC×GC). The RGA is a gas chromatograph used to

quantify the smallest components, including N_2, H_2 and hydrocarbons with up to 4 carbon atoms. Detection is done using two thermal conductivity detectors and one flame ionization detector. The majority of the products and the surrogate components were detected with GC×GC. Detection was done with a flame ionization detector for quantification of the product species and with a quadrupole mass spectrometer for product identification. For quantification of the effluent mass fractions of the smallest molecules detected with the RGA, N_2 is used as an internal standard. Calibration is performed with a calibration mixture provided by Air Liquide. For the larger molecules detected with GC×GC, methane is used as a secondary internal standard and the effective carbon number approach is used to calculate product mass fractions. The relative experimental error on the calculated mass fractions with this method is 7% based on experience.

5. Surrogate model validation

The full kinetic model is used for comparison against (1) the new aromatic-enriched surrogate pyrolysis experiments performed at Ghent University in a tubular reactor and (2) shock-tube experiments of Jet A pyrolysis reported by Han et al.[8] The surrogate experiments are used to evaluate the completeness and importance of the cross-chemistry generated by RMG.

Besides the newly developed kinetic model, the HyChem model that was recently published by Wang et al.[3] and Xu et al.[4] is also used to simulate the experimental data. The HyChem model is a lumped kinetic model that combines a base mechanism with only 7 reactions covering fuel pyrolysis and oxidation. A comparison of the model simulations with the new experimental data and the experimental data published by Han et al.[8] is given in Supporting Information. A decent model performance is obtained given that the HyChem model is developed for a specific Jet A fuel with a slightly different composition than the one used in this experimental work. Especially for the prediction of aromatics, but also for other major product species, the new detailed kinetic model outperforms the lumped HyChem model.

5.1. Comparison against surrogate pyrolysis experiments

The new surrogate pyrolysis experiments are simulated using the 1-D plug flow reactor implementation in CHEMKIN.[33] The temperatures profiles that are measured experimentally as a function of the axial reactor coordinate are used as input to CHEMKIN, together with the experimentally measured feedstock composition, flow rates, and pressure. The model simulations are compared against the experimental measurements of the main products in Figure 4.

The conversion of the main surrogate components, *n*-dodecane, isooctane, and *n*-propyl benzene are predicted well by the model. For the minor surrogate component TMB, the onset of conversion is predicted well, but the model overpredicts the fuel conversion at higher temperatures. Potential reasons for this discrepancy are discussed further. The main products that are experimentally measured are those expected from typical pyrolysis experiments, *i.e.* methane, ethene, propene, benzene, and toluene. Additionally, isobutene and styrene are measured with high mass fractions. The model captures the trend of all major product species as a function of temperature and can predict absolute product mass fractions with a good accuracy for all the main products. The main discrepancy is found for styrene, which is underpredicted by a factor 1.5 approximately. The plateau in the propene mass fraction at higher temperatures is not well captured by the model. This plateau is most likely the result of the interplay between hydrogen atom addition reactions to propene to form either 1-propyl radicals or 2-propyl radicals. The former can further react back to propene or decompose to ethene and methyl radicals. The latter reaction channel typically becomes more important at higher temperatures. Refining the rate coefficients for these reactions with high-accuracy calculations will likely improve the prediction of propene at higher temperatures.

The final model used for simulations is slightly modified from the model automatically generated by RMG. The models generated for the pure surrogate components were each validated against literature experimental data for the pyrolysis of those pure components, when available. The new experimental data on surrogate pyrolysis is used to screen the completeness and accuracy of the cross-chemistry that is automatically generated by RMG. The rate-of-production analysis, discussed in more detail further, demonstrates the importance of cross-chemistry in multi-component mixtures. It is found that the initial resonantly stabilized radical formed from TMB, further referred to as R_{TMB}, has no obvious unimolecular decomposition channels since unimolecular decomposition would imply breaking of the aromatic structure. The accumulation of this radical makes it the most important abstracting radical for the other surrogate components. The most important hydrogen abstraction reactions by R_{TMB} from *n*-dodecane, *n*-propyl benzene and isooctane were found automatically by RMG, whilst some hydrogen abstraction reactions from the less important sites were not considered. Manual addition of those with rate coefficients determined by RMG improved the model performance to the state that is shown in Figure 4. For some of the reactions with R_{TMB}, the automatically calculated reaction path degeneracy was corrected by a factor of 2. Note that besides small corrections to the reaction path degeneracy, none

of the thermodynamic properties or rate coefficients generated by RMG are adjusted in the final model.

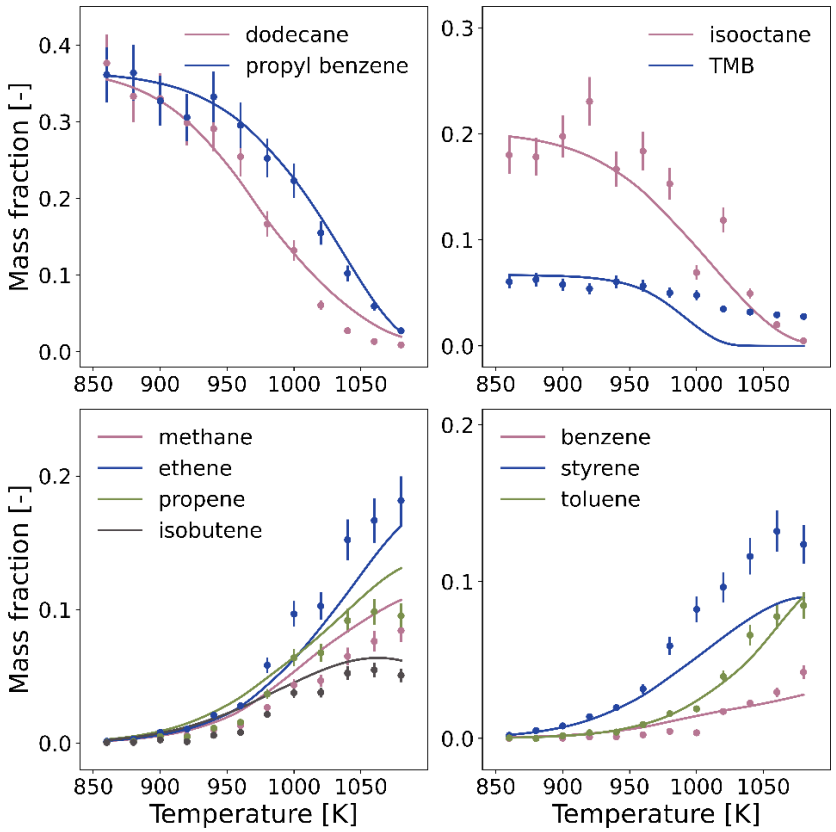

Figure 4. Comparison of simulations with the full kinetic model against the new experimental data of surrogate pyrolysis measured in a tubular reactor.

5.2. Comparison against Jet A pyrolysis

To evaluate to which extent the surrogate mixture can be used to model the pyrolysis of a commercial Jet A fuel, additional simulations with the adjusted full kinetic model from section 5.1 are done and compared to Jet A pyrolysis experiments. The experimental data reported by Han et al.[8] is used for comparison. Those experiments are done in a shock tube at 25 and 90 atm, for temperature ranging from 900 to 2200 K, and an average residence time of 2.3 ms. The post-shock experimental composition is compared with CHEMKIN simulations using the batch reactor implementation and the full kinetic model. The comparison of experimental measurements and model simulations at 25 atm are given in Figure 5, the comparison at 90 atm is given in Figure S4 of the Supporting Information.

The major products formed by the pyrolysis of the commercial Jet A fuel in a shock tube reactor are light hydrocarbons (methane, ethane, ethene, ethyne, and propene) and simple aromatics (benzene and toluene). The experimentally measured mole fractions (ppm) of those products are given in Figure 5 as a function of temperature. For simulations, Jet A is represented by the surrogate composition reported by Dooley et al.[12] with 21.13 ppm *n*-dodecane, 15.01 ppm isooctane, 12.29 ppm *n*-propyl benzene, and 3.87 ppm TMB, diluted in Ar. Giving that the jet fuel is represented by a surrogate rather than its detailed composition, a good predictive ability of the model is observed for the major product species. Even though the mole fractions of some products are slightly over- or underpredicted, the general trends and quantities of the major product species are captured well.

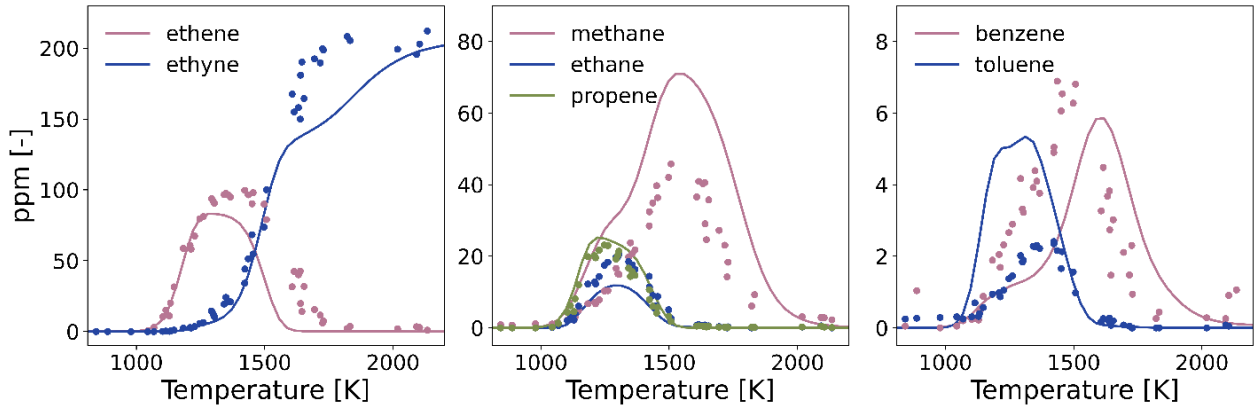

Figure 5. Comparison of simulations with the full kinetic model against shock tube experimental data for the pyrolysis of commercial Jet A in a shock tube study at 25 atm reported by Han et al. [8]

6. Model analysis

6.1. Rate-of-production analysis

To further analyze the complete kinetic model and empathize the importance of cross-reactions, a rate-of-production analysis is performed. The rate-of-production analysis is done using the batch reactor implementation in CHEMKIN with the previously defined surrogate composition, at 950 K, 1000 K, and 1050 K, 3 bar and a residence time of 0.01 s. The low residence time is selected to focus the rate-of-production analysis on initial decomposition pathways of the different surrogate components. The other conditions are selected based on the conditions used for the experimental measurements in the tubular reactor.

The most important initial decomposition chemistry is schematically represented in Figure 6, together with the relative production rates of those reactions. The relative production rates are defined as the production rate of that reaction relative to the net production rate of the surrogate component from which that reaction originates. The values are determined at 950 K, 1000 K, and 1050 K (italic, bold, and normal font in Figure 6). A brief description of the most important chemistry is given below.

The first surrogate component to consider is 1,3,5-trimethylbenzene (TMB). At 0.01 s residence time, TMB has a molar conversion of 2.6%, 13%, and 59% for 950 K, 1000 K, and 1050 K respectively. At all investigated conditions, TMB is primarily consumed by hydrogen abstraction reactions by methyl radicals. Hydrogen abstraction reactions by other radicals (e.g. hydrogen atoms, ethyl radicals, and phenyl radicals) play a minor role. The formed radical from TMB (R_{TMB}) cannot easily decompose by a unimolecular reaction and becomes the main abstracting species in the overall decomposition scheme. This phenomenon demonstrates the importance of cross-chemistry for complex multi-component feedstocks. As a large fraction of R_{TMB} reacts back to TMB, the relative rate of production for the hydrogen abstraction reaction of TMB by methyl radicals is 4071%, 998%, and 216% at 950 K, 1000 K, and 1050 K respectively. R_{TMB} mainly acts as an abstracting agent for the other surrogate components, *n*-dodecane, isooctane, and *n*-propyl benzene. The relative rate of production is given in Figure 6. Alternatively, R_{TMB} can abstract hydrogen atoms from major product species (e.g. propene and isobutene). The contribution of the hydrogen abstraction from other product species increases with increasing temperature, *i.e.* increasing conversion, and hence a higher product concentration. The overall role of R_{TMB} as an abstracting species diminishes with increasing temperatures. At higher temperatures, the radical concentration in the mixture increases and R_{TMB} can react further by recombination with allyl or isobutene-3-yl radicals. Alternatively, R_{TMB} reacts by addition to saturated products, such as ethene. The discrepancy in the TMB mass fraction in Figure 4 is most likely due to an overestimation of the recombination reaction rates or uncertainty in the thermodynamic properties of the products. The faster consumption of R_{TMB} by alternative reactions reduces the fraction of R_{TMB} that reacts by hydrogen abstraction reactions back to TMB.

The second surrogate component, *n*-dodecane, has a molar conversion of 6.6%, 27%, 62% at 0.01 s and 950 K, 1000 K, and 1050 K respectively. *n*-dodecane is mainly consumed by hydrogen abstraction reactions with the formation of five different secondary radicals. For simplicity, only

one of those radicals, the one with the highest flux, is given in Figure 6. The main abstracting species at 950 K and 1000 K is R_{TMB} and shifts to methyl radicals at the highest temperature of 1050 K. At higher temperatures, the contribution of homolytic C-C scission reactions for the consumption of *n*-dodecane increases, but hydrogen abstraction reactions remain the most important consumption channels at the temperatures considered. The secondary radicals formed from *n*-dodecane react further by β-scission reactions, with the formation of a 1-alkene and a primary radical (propene and 1-nonyl in Figure 6). The primary radical reacts by a hydrogen shift reaction through a 5- or 6-membered cyclic transition state structure with the formation of another secondary radical. Those secondary radicals decompose by β-scission reactions or new hydrogen shifts. The 1-alkene products formed from the β-scission reactions, for example 1-hexene in Figure 6, are further consumed by hydrogen atom addition to the double bond or by homolytic C-C scission with the formation of an allyl and primary radical. Overall, the consumption of the 1-alkene products increases with increasing temperatures.

The molar conversion of isooctane at 0.01 s is 4.6%, 14%, and 53% for 950 K, 1000 K, and 1050K respectively. Isooctane can form four different radicals by hydrogen abstraction reactions. The three radicals that are formed with the highest rate of production are given in Figure 6. Their relative importance depends on the considered temperature. Additionally, isooctane reacts by homolytic C-C scission reactions. The importance of latter channel increases with increasing temperatures and the relative rate of production goes up to 22% at 1050 K. The main radical formed after hydrogen abstraction from isooctane is a tertiary radical. This radical decomposes by a β-scission reaction with the formation of isobutene and a tertiary isobutyl radical. The latter radical can form another isobutene molecule by C-H β-scission, or isomerize to a primary isobutyl radical that further decomposes to propene and a methyl radical. Hydrogen abstraction from isooctane can also produce a primary and secondary radical, as indicated in Figure 6. Both decompose further by β-scission reactions. The unsaturated products formed after β-scission react further similar to the 1-alkenes formed as part of *n*-dodecane consumption, *i.e.* by hydrogen atom addition to the double bond or by a homolytic scission with the formation of a resonantly stabilized radical.

The last surrogate component, *n*-propyl benzene, has a molar conversion of 3.1%, 14%, and 39% at 950 K, 1000 K, and 1050 K respectively and a residence time of 0.01 s. *n*-propyl benzene has three main decomposition channels: (i) homolytic C-C bond scission with the formation of a phenyl radical and an ethyl radical, (ii) hydrogen abstraction reaction resulting in three different

radicals, only the resonantly stabilized radical with the highest rate of formation is presented in Figure 6, and (iii) hydrogen atom addition and simultaneous β-scission with the formation of benzene and a 1-propyl radical. The importance of the homolytic bond scission increases with increasing temperatures, but the main decomposition channels are hydrogen abstraction reactions. Similar to *n*-dodecane and isooctane, the main abstracting species is R_{TMB} at the lowest temperatures and shifts to methyl radicals at the highest temperature studied. The majority of hydrogen abstraction reactions results in the formation of a resonantly stabilized radical that can further decompose by a β-scission reaction to styrene and methyl radicals. Alternatively, and with increasing importance at higher temperatures, abstraction reactions result in the formation of a primary radical that can react further to ethylene and a phenyl radical. The formed phenyl radicals are important abstracting agents for the surrogate molecules and main products formed.

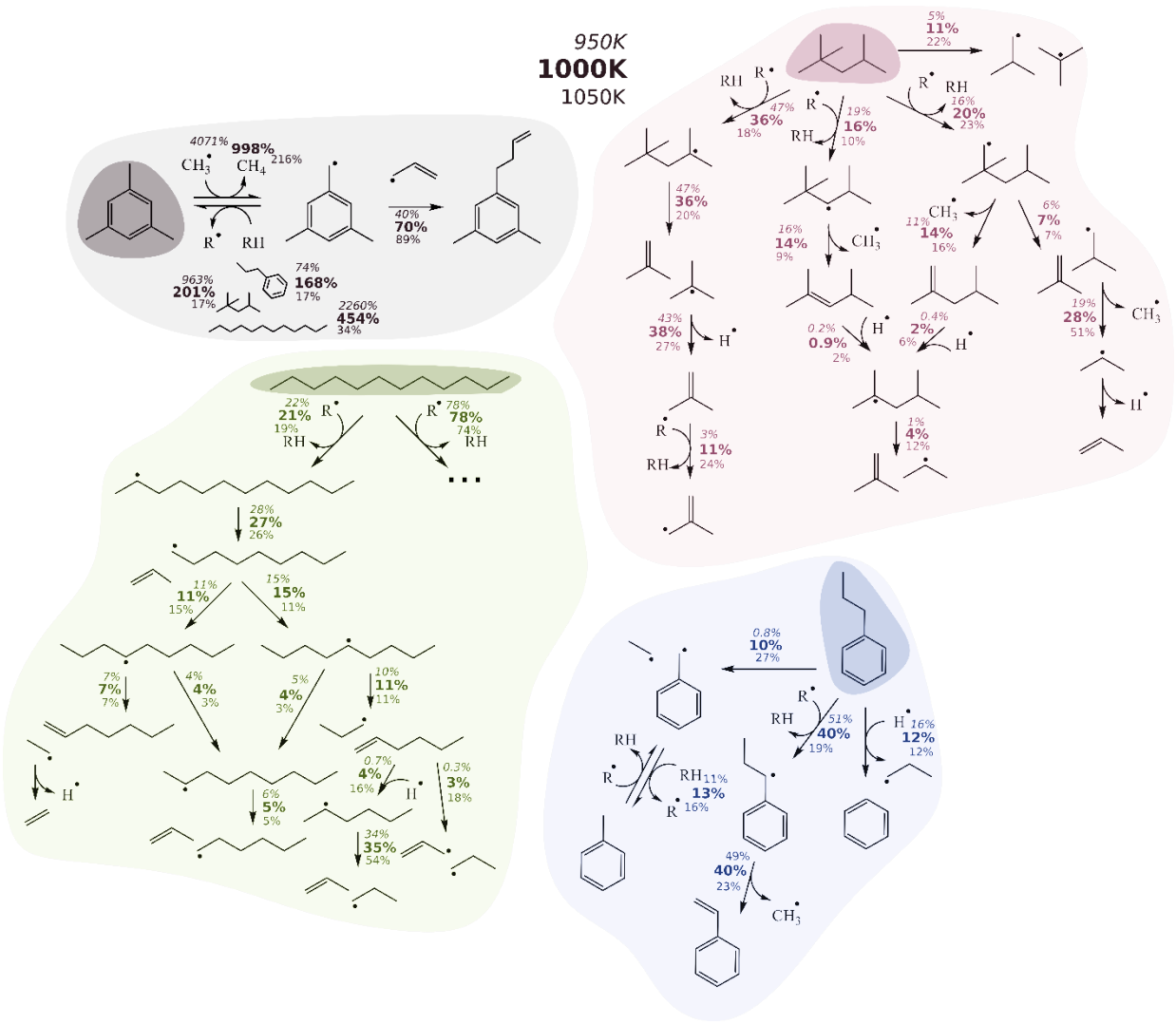

Figure 6. Rate-of-production analysis for the initial decomposition of the surrogate mixture. Simulations are done in a batch reactor at 3 bar, for a residence time of 0.01 s, and with the predefined surrogate mixture composition. Reported numbers are the relative rate of production of the reactions with respect to the rate of production of their respective starting surrogate component at 950 K (italic), 1000 K (bold), and 1050 K (normal font).

6.2. Sensitivity analysis

The rate-of-production analysis clearly demonstrates the importance of cross-chemistry when dealing with a multi-component surrogate mixture. To further analyze the importance of cross-chemistry, sensitivity analysis is done for the pre-exponential factors using the batch reactor implementation in CHEMKIN. The conditions used for the sensitivity analysis are similar to those used for the rate of production analysis. The pressure in the reactor is set to 3 bar, the temperature to 1000 K, and the residence time is fixed at 0.01 s. The most sensitive reactions with respect to the surrogate components are compared for simulations done with the surrogate mixture and for

the decomposition of the pure surrogate components. For example, the most sensitive reactions for isooctane are compared for isooctane as part of the surrogate mixture and for the thermal decomposition of pure isooctane at the same conditions. For all four surrogate components, the most sensitive reactions are selected and presented in Figure 7. The blue bars in Figure 7 indicate the normalized sensitivity coefficients during decomposition of the component as part of the surrogate mixtures. The orange bars in Figure 7 indicate the normalized sensitivity coefficients during decomposition of the pure component. Positive sensitivity coefficients mean that increasing the pre-exponential factor of that reaction results in an increase of the surrogate component concentration, while a negative sensitivity coefficient suggests a decrease in the component's concentration.

For all surrogate components, it is clear from Figure 7 that the sensitive reactions differ between the pure component decomposition and the decomposition of that component in a multi-component surrogate mixture. Moreover, many of the sensitive reactions are reactions originating from other surrogate components rather than the one investigated. For example, the homolytic scission reaction of isooctane to a primary and tertiary isobutyl radical is a sensitive reaction for all surrogate components. Also, reactions between different surrogate components are found as sensitive reactions, for example the hydrogen abstraction reaction by R_{TMB} appears in the sensitivity analysis for each of the surrogate components. Many of the reactions appearing in the sensitivity analysis are initial decomposition reactions of that surrogate component or reactions that increase or reduce the number of radicals in the system. The most sensitive reactions for each of the surrogate components are shortly discussed below.

For isooctane decomposition, the most sensitive reactions are similar for the decomposition of isooctane as part of a surrogate mixture or as a pure component. Those reactions are homolytic scission reactions of isooctane and hydrogen abstraction reactions from isooctane by hydrogen atoms and methyl radicals. Hydrogen abstraction reactions by R_{TMB} are sensitive only during the surrogate decomposition. One reaction with a positive sensitivity coefficient for the decomposition of isooctane as a single component is the recombination reaction of methyl radicals. This reaction reduces the radical concentration, so leads to a lower conversion of isooctane, and hence has a positive sensitivity coefficient. This reaction is not as sensitive for isooctane in the surrogate decomposition, since methyl radicals are consumed by hydrogen abstraction reactions by other surrogate components (e.g. TMB), such that their recombination decreases in importance.

n-propyl benzene and *n*-dodecane are both sensitive to the homolytic scission of isooctane and the reaction of those components with R_{TMB} for the decomposition in the surrogate mixture. In both cases the sensitive reactions are rather different between the decomposition of the pure components and in the surrogate mixture. In both cases, positive sensitivity coefficients are observed for consumption channels of methyl radicals though recombination reactions, for example, the recombination of methyl and phenyl radicals or the recombination of methyl and ethyl radicals.

At the selected reactor conditions, the conversion of pure TMB is low (<1%). As a result, there are no sensitive reactions and only the sensitive reactions for decomposition as part of the surrogate mixture are presented in Figure 7. Similar to *n*-propyl benzene and *n*-dodecane, TMB is sensitive to the homolytic scission reactions of isooctane. Furthermore, reactions involving TMB and R_{TMB} are part of the sensitive reactions. Usually, the hydrogen abstraction reactions from the fuel component and homolytic bond scission of the fuel component have a negative sensitivity coefficient since those reactions lead to the consumption of the surrogate component. However, for some cases the opposite is true for TMB decomposition. As explained in the rate-of-production analysis, the radical formed from TMB, *i.e.* R_{TMB}, is the main abstracting radical in the surrogate mixture because of the lack of further unimolecular decomposition reactions. After hydrogen abstraction or recombination with hydrogen atoms, R_{TMB} reacts back to TMB, resulting in a positive sensitivity coefficient for some of the sensitive reactions.

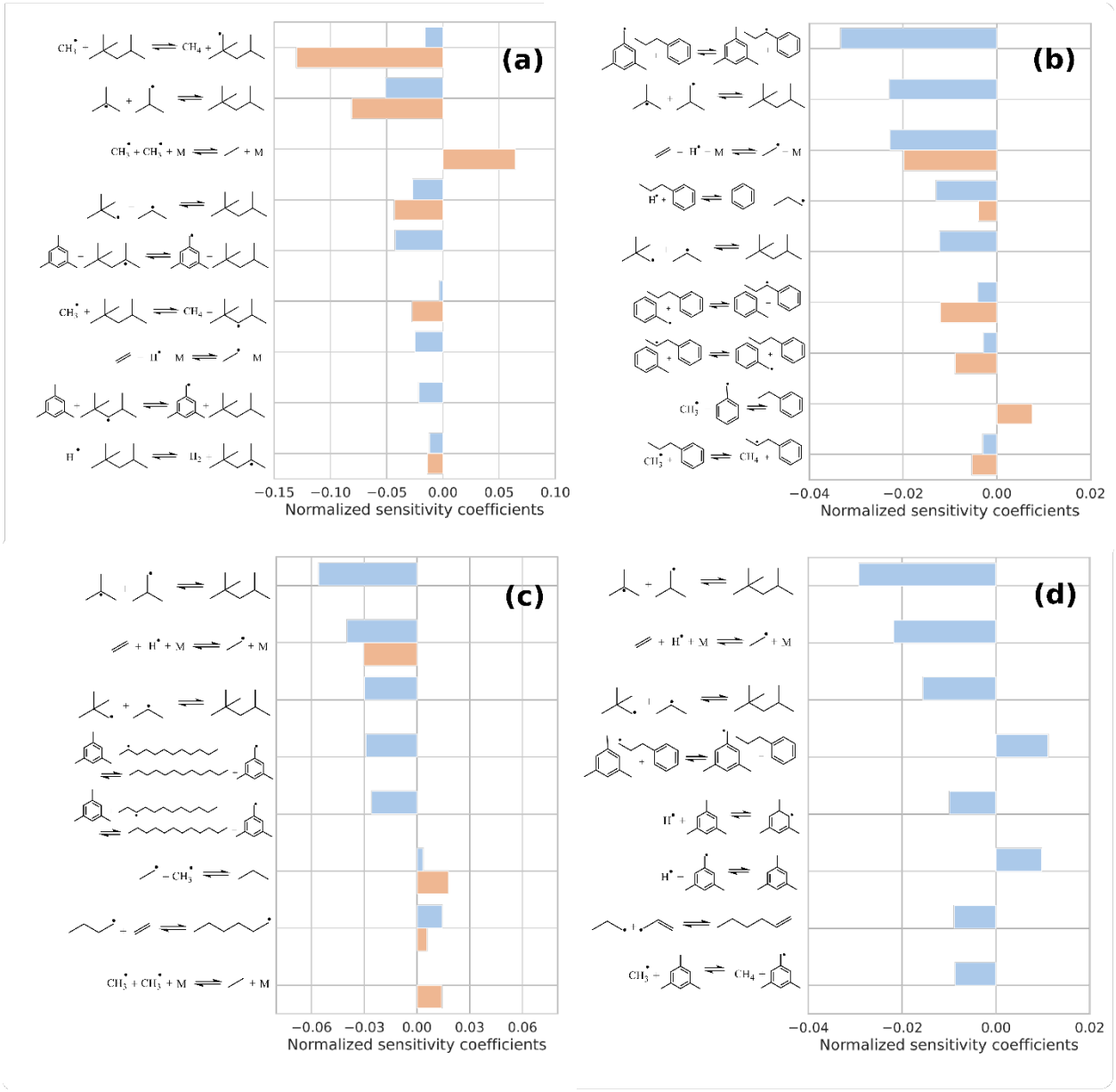

Figure 7. Normalized sensitivity coefficients with respect to the four different surrogate components (a) isooctane, (b) *n*-propyl benzene, (c) *n*-dodecane, and (d) 1,3,5-trimethylbenzene. Simulations are done in a batch reactor at 3 bar, 1000 K, and 0.01 s residence time. The sensitive reactions for the predefined surrogate composition (blue bars) are compared to those for pure component decomposition (orange bars).

7. Conclusions

A detailed kinetic model for the pyrolysis of a Jet A surrogate is developed with the automatic kinetic model generation tool RMG. This is the first reported kinetic model for Jet A pyrolysis with this high level of chemical detail. Additionally, new experimental data for the pyrolysis of a Jet A surrogate are gathered in a tubular reactor with a dedicated analysis section. Model analysis

techniques are employed to demonstrate the importance of cross-chemistry during pyrolysis of multi-component mixtures.

RMG is used for the generation of a kinetic model for a multi-component mixture, not by feeding the complete surrogate mixture to RMG, which results in an explosion of the number of generated species and reactions, but in a stepwise approach, easily applicable to similarly complex systems. The construction starts with the generation of single component kinetic models for *n*-dodecane, isooctane, *n*-propyl benzene, and 1,3,5-trimethylbenzene pyrolysis. Those models are each validated against literature experimental data and the RMG databases are updated with more accurate CBS-QB3 calculations to achieve good model performance. Next, the cross-chemical reactions are automatically generated with RMG and all models are merged together.

The final kinetic model is validated against the new experimental data for surrogate pyrolysis in a tubular reactor, and against the pyrolysis of a commercial Jet A in a shock tube reactor. In both cases good agreement is achieved between model simulation and experimental product profiles. Similar model performance is expected for pressures, temperatures, residence times, and surrogate compositions within the range that is validated against experimental data. This includes temperatures between 860 and 2200 K, pressures from atmospheric up to 90 atm, and residence times ranging from the order of milliseconds up to seconds. The good performance for different reactor geometries, experimental conditions, and fuel or surrogate composition, demonstrate the uniqueness of the novel kinetic model in its wide applicability caused by the high level of chemical detail.

The chemical detail allows for further analysis of the important chemistry during the thermal decomposition of the surrogate mixture. Both the rate-of-product analysis and sensitivity analysis highlight the importance of cross-chemical reaction between the different surrogate components. The initial radical formed from 1,3,5-trimethylbenzene lacks unimolecular decomposition channels at the investigated conditions and acts as the main abstracting agent for the other surrogate components and the main products formed.

Supporting information

The supporting information of this work includes the newly developed kinetic model (*SI_chem_model.inp*), a list of species identifiers for this model (*SI_species_identifiers.csv*), and details on the new experimental data (*SI_exp_data.xlsx*). Additional comparisons of the new kinetic model and the HyChem kinetic model to literature experimental data are provided.

Acknowledgements

We gratefully acknowledge Mitsubishi Heavy Industries for financial support for this research. The research leading to these results has received funding from the Fund for Scientific Research Flanders (FWO) and European Research Council under the European Union's Horizon 2020 research and innovation program / ERC grant agreements n° 818607 'ERC OPTIMA'. Florence Vermeire acknowledges the Belgian American Educational Foundation (B.A.E.F.) for funding of her postdoctoral fellowship. Agnes Jocher acknowledges financial support from the DFG Research Fellowship under JO 1526/1-1. We thank Marko Djokic for his support and advice during the experiments.

References

(1) Ning, W.;Yu, P.;Jin, Z. Research Status of Active Cooling of Endothermic Hydrocarbon Fueled Scramjet Engine. *Proc. Inst. Mech. Eng. Part G J. Aerosp. Eng.* **2013**, *227* (11), 1780–1794. https://doi.org/10.1177/0954410012463642.

(2) Daniau, E.;Sicard, M. Experimental and Numerical Investigations of an Endothermic Fuel Cooling Capacity for Scramjet Application. *A Collect. Tech. Pap. - 13th AIAA/CIRA Int. Sp. Planes Hypersonic Syst. Technol. Conf.* **2005**, *3*, 1808–1816. https://doi.org/10.2514/6.2005-3404.

(3) Wang, H.;Xu, R.;Wang, K.;Bowman, C. T.;Hanson, R. K.;Davidson, D. F.;Brezinsky, K.;Egolfopoulos, F. N. A Physics-Based Approach to Modeling Real-Fuel Combustion Chemistry - I. Evidence from Experiments, and Thermodynamic, Chemical Kinetic and Statistical Considerations. *Combust. Flame* **2018**, *193*, 502–519. https://doi.org/10.1016/j.combustflame.2018.03.019.

(4) Xu, R.;Wang, K.;Banerjee, S.;Shao, J.;Parise, T.;Zhu, Y.;Wang, S.;Movaghar, A.;Lee, D.

J.;Zhao, R.;et al. A Physics-Based Approach to Modeling Real-Fuel Combustion Chemistry – II. Reaction Kinetic Models of Jet and Rocket Fuels. *Combust. Flame* **2018**, *193*, 520–537. https://doi.org/10.1016/j.combustflame.2018.03.021.

(5) Gao, C. W.;Allen, J. W.;Green, W. H.;West, R. H. Reaction Mechanism Generator: Automatic Construction of Chemical Kinetic Mechanisms. *Comput. Phys. Commun.* **2016**, *203*, 212–225. https://doi.org/10.1016/j.cpc.2016.02.013.

(6) Liu, M.;Grinberg Dana, A.;Johnson, M. S.;Goldman, M. J.;Jocher, A.;Payne, A. M.;Grambow, C. A.;Han, K.;Yee, N. W.;Mazeau, E. J.;et al. Reaction Mechanism Generator v3.0: Advances in Automatic Mechanism Generation. *J. Chem. Inf. Model.* **2021**, *61* (6), 2686–2696. https://doi.org/10.1021/acs.jcim.0c01480.

(7) Malewicki, T.;Gudiyella, S.;Brezinsky, K. Experimental and Modeling Study on the Oxidation of Jet A and the N-Dodecane/Iso-Octane/n-Propylbenzene/1,3,5-Trimethylbenzene Surrogate Fuel. *Combust. Flame* **2013**, *160* (1), 17–30. https://doi.org/10.1016/j.combustflame.2012.09.013.

(8) Han, X.;Liszka, M.;Xu, R.;Brezinsky, K.;Wang, H. A High Pressure Shock Tube Study of Pyrolysis of Real Jet Fuel Jet A. *Proc. Combust. Inst.* **2019**, *37* (1), 189–196. https://doi.org/10.1016/j.proci.2018.05.136.

(9) Colket, M.;Edwards, T.;Williams, S.;Cernansky, N. P.;Miller, D. L.;Egolfopoulos, F.;Dryer, F. L.;Bellan, J.;Lindstedt, P.;Seshadri, K.;et al. Identification of Target Validation Data for Development of Surrogate Jet Fuels. *46th AIAA Aerosp. Sci. Meet. Exhib.* **2008**, 1–12. https://doi.org/10.2514/6.2008-972.

(10) Dryer, F. L.;Jahangirian, S.;Dooley, S.;Won, S. H.;Heyne, J.;Iyer, V. R.;Litzinger, T. A.;Santoro, R. J. Emulating the Combustion Behavior of Real Jet Aviation Fuels by Surrogate Mixtures of Hydrocarbon Fluid Blends: Implications for Science and Engineering. *Energy and Fuels* **2014**, *28* (5), 3474–3485. https://doi.org/10.1021/ef500284x.

(11) Dooley, S.;Won, S. H.;Chaos, M.;Heyne, J.;Ju, Y.;Dryer, F. L.;Kumar, K.;Sung, C. J.;Wang, H.;Oehlschlaeger, M. A.;et al. A Jet Fuel Surrogate Formulated by Real Fuel Properties. *Combust. Flame* **2010**, *157* (12), 2333–2339.

https://doi.org/10.1016/j.combustflame.2010.07.001.

(12) Dooley, S.;Won, S. H.;Heyne, J.;Farouk, T. I.;Ju, Y.;Dryer, F. L.;Kumar, K.;Hui, X.;Sung, C. J.;Wang, H.;et al. The Experimental Evaluation of a Methodology for Surrogate Fuel Formulation to Emulate Gas Phase Combustion Kinetic Phenomena. *Combust. Flame* **2012**, *159* (4), 1444–1466. https://doi.org/10.1016/j.combustflame.2011.11.002.

(13) RMG - Reaction Mechanism Generator.

(14) Han, K.;Jamal, A.;Grambow, C. A.;Buras, Z. J.;Green, W. H. An Extended Group Additivity Method for Polycyclic Thermochemistry Estimation. *Int. J. Chem. Kinet.* **2018**, *50* (4), 294–303. https://doi.org/10.1002/kin.21158.

(15) Lai, L.;Khanniche, S.;Green, W. H. Thermochemistry and Group Additivity Values for Fused Two-Ring Species and Radicals. *J. Phys. Chem. A* **2019**, *123* (15), 3418–3428. https://doi.org/10.1021/acs.jpca.9b01065.

(16) Montgomery, J. A.;Frisch, M. J.;Ochterski, J. W.;Petersson, G. A. A Complete Basis Set Model Chemistry. VI. Use of Density Functional Geometries and Frequencies. *J. Chem. Phys.* **1999**, *110* (2–12), 2822–2827. https://doi.org/10.1063/1.477924.

(17) Montgomery, J. A.;Frisch, M. J.;Ochterski, J. W.;Petersson, G. A. A Complete Basis Set Model Chemistry. VII. Use of the Minimum Population Localization Method. *J. Chem. Phys.* **2000**, *112* (15), 6532–6542. https://doi.org/10.1063/1.481224.

(18) Green, W. H. Chapter 5 - Automatic Generation of Reaction Mechanisms. In *Mathematical Modelling of Gas-Phase Complex Reaction Systems: Pyrolysis and Combustion*; Faravelli, T., Manenti, F., Ranzi, E., Eds.; Elsevier, 2019; Vol. 45, pp 259–294. https://doi.org/10.1016/B978-0-444-64087-1.00005-X.

(19) Green, W. H. Moving from Postdictive to Predictive Kinetics in Reaction Engineering. *AIChE J.* **2020**, *66* (11), e17059. https://doi.org/10.1002/aic.17059.

(20) Gudiyella, S.;Brezinsky, K. The High Pressure Study of N-Propylbenzene Pyrolysis. *Proc. Combust. Inst.* **2013**, *34* (1), 1767–1774. https://doi.org/10.1016/j.proci.2012.05.007.

(21) Darcy, D.;Tobin, C. J.;Yasunaga, K.;Simmie, J. M.;Würmel, J.;Metcalfe, W. K.;Niass, T.;Ahmed, S. S.;Westbrook, C. K.;Curran, H. J. A High Pressure Shock Tube Study of N-

Propylbenzene Oxidation and Its Comparison with n-Butylbenzene. *Combust. Flame* **2012**, *159* (7), 2219–2232. https://doi.org/10.1016/j.combustflame.2012.02.009.

(22) Frisch, M. J.;Trucks, G. W.;Schlegel, H. B.;Scuseria, G. E.;Robb, M. a.;Cheeseman, J. R.;Scalmani, G.;Barone, V.;Petersson, G. a.;Nakatsuji, H.;et al. G16_C01. 2016, p Gaussian 16, Revision C.01, Gaussian, Inc., Wallin.

(23) Allen, J. W.;Goldsmith, C. F.;Green, W. H. Automatic Estimation of Pressure-Dependent Rate Coefficients. *Phys. Chem. Chem. Phys.* **2012**, *14* (3), 1131–1155. https://doi.org/10.1039/C1CP22765C.

(24) Grinberg Dana, A.;RMG Team. Automated Reaction Kinetics and Network Exploration (Arkane). 2020.

(25) Chen, Q.;Froment, G. F. Thermal Cracking of Substituted Aromatic Hydrocarbons. II. Kinetic Study of the Thermal Cracking of n-Propylbenzene and Ethylbenzene. *J. Anal. Appl. Pyrolysis* **1991**, *21* (1), 51–77. https://doi.org/10.1016/0165-2370(91)80015-Z.

(26) Herbinet, O.;Marquaire, P. M.;Battin-Leclerc, F.;Fournet, R. Thermal Decomposition of N-Dodecane: Experiments and Kinetic Modeling. *J. Anal. Appl. Pyrolysis* **2007**, *78* (2), 419–429. https://doi.org/10.1016/j.jaap.2006.10.010.

(27) Malewicki, T.;Brezinsky, K. Experimental and Modeling Study on the Pyrolysis and Oxidation of N-Decane and n-Dodecane. *Proc. Combust. Inst.* **2013**, *34* (1), 361–368. https://doi.org/10.1016/j.proci.2012.06.156.

(28) Malewicki, T.;Comandini, A.;Brezinsky, K. Experimental and Modeling Study on the Pyrolysis and Oxidation of Iso-Octane. *Proc. Combust. Inst.* **2013**, *34* (1), 353–360. https://doi.org/10.1016/j.proci.2012.06.137.

(29) Liu, M.;Chu, T.-C.;Jocher, A.;Smith, M. C.;Lengyel, I.;Green, W. H. Predicting Polycyclic Aromatic Hydrocarbon Formation with an Automatically Generated Mechanism for Acetylene Pyrolysis. *Int. J. Chem. Kinet.* **2021**, *53* (1), 27–42. https://doi.org/10.1002/kin.21421.

(30) Harper, M. R.;Van Geem, K. M.;Pyl, S. P.;Marin, G. B.;Green, W. H. Comprehensive Reaction Mechanism for N-Butanol Pyrolysis and Combustion. *Combust. Flame* **2011**, *158* (1), 16–41. https://doi.org/10.1016/j.combustflame.2010.06.002.

(31) Pyl, S. P.;Schietekat, C. M.;Van Geem, K. M.;Reyniers, M.-F.;Vercammen, J.;Beens, J.;Marin, G. B. Rapeseed Oil Methyl Ester Pyrolysis: On-Line Product Analysis Using Comprehensive Two-Dimensional Gas Chromatography. *J. Chromatogr. A* **2011**, *1218* (21), 3217–3223. https://doi.org/10.1016/j.chroma.2010.12.109.

(32) De Bruycker, R.;Anthonykutty, J. M.;Linnekoski, J.;Harlin, A.;Lehtonen, J.;Van Geem, K. M.;Räsänen, J.;Marin, G. B. Assessing the Potential of Crude Tall Oil for the Production of Green-Base Chemicals: An Experimental and Kinetic Modeling Study. *Ind. Eng. Chem. Res.* **2014**, *53* (48), 18430–18442. https://doi.org/10.1021/ie503505f.

(33) ANSYS Inc. Chemkin-Pro 18.2. San Diego 2017.